Depth estimation of gravity anomalies using Artificial Neural Networks

Alireza Hajian[1],Vahid Ebrahimzadeh Ardestani[2],Zahra Ziaee[3]
Email:a_hajian@yahoo.com

Abstract:

The method of Artificial Neural Networks is used as a suitable tool for intelligent interpretation of gravity data in exploration; in this paper, we have designed a Hopfield Neural Network to estimate the gravity source depth. To calculate the weights and biasing values of the network first the network is designed for the models near to sphere or cylinder and these weights are fixed and the network will rotate so that finally get to its stable state . In this state the energy of the network will be in its minimum value. Thus the network will run for some different initial values of depths and the one which will have the least final energy will finally the depth of gravity source. It is very important to test the designed network we fed the noisy data to it and observed its behavior.

This Artificial Neural network was used to estimate the depth of a qanat in north entrance of the Geophysics Institute of Tehran University and the result was very near to the real value of depth.

Keywords: Artificial neural network, Gravity Exploration, Depth estimation,Hopefield

1-Introduction:

Neural Networks are increasingly being used in prediction, estimation, and optimization problems. Neural networks have gained in popularity in geophysics this last decade.

They have been applied successfully to a variety of problems in geophysics. Nowadays Neural Networks can be applied in microchip technology for computer hardware.

Recent developments in gravity measurements and especially in microgravity tools has been prepaid an excellent conditions of data acquisition to have better interpretation results specially depth estimation of gravity sources.

These developments, combined with higher speed data acquisition technology, have made it possible to detect much smaller objects like small cavities, chromites lenses, etc.

The gravity data sets are naturally noisy so that it is very hard to estimate the gravity source depths precisely. Therefore, there is an increasingly need for a fully automatic interpretation technique that can be used to make decisions regarding the nature of the sources in real time. The massively parallel processing advantage of Artificial Neural Networks makes them suitable for hardware implementation; therefore, the detection of small gravity sources objects will be possible more precisely.

However, gravity and specially microgravity data measurements create a large amount of data which needs to some corrections and filtering like: tidal correction, drift correction, latitude correction ,free air correction ,up-ward or down-ward continuation , etc that need to be analyzed and interpreted and this can be time consuming and results mostly have not good adaptations to real values .Therefore there is an increasing need for intelligent interpretation techniques that can be used to make rapid decisions in the field during operations .Specially its very important to mention that some techniques like Euler method ,Analytical signal ,up-ward continuation and

[1]Student of MSc. in Geophysics Institute of Tehran University
[2] DR. of Geophysics in Geophysics Institute of Tehran University
[3] MSc. of computer ,IT head of Industries and Mines ministry

down-ward continuation are very sensitive to noise and can estimate only the edges or around of the gravity source location.

So we need a technique not very sensitive to noise and more precise for depth estimation of gravity anomalies.

One such technique may be found in the emerging field of Artificial Neural Networks.

In this paper, we have developed a new method for detection and depth estimation of gravity anomalies using Hopfield Neural Network applied to gravity data.

The Hopfield networks have already been electrically and electro-optically implemented. Therefore, we can use these chips in future generations of gravimeters instrumentations

2-Artificial Neural Networks

Artificial neural networks are part of much wider field called artificial intelligence, which can be defined as the study of mental facilities through the use of computational models (Charniak and McDermott.1985).There are several types of artificial neural networks .For a complete information covering the whole domain of neural networks kinds, the reader is referred to the excellent book of Fundamental of Artificial Neural Networks by Menhaj(2000).

Summarizing their reviews, neural networks can be divided into two main categories: supervised feed-forward networks and unsupervised recurrent networks .In the supervised feed-forward, information is only allowed to flow in one direction without any feedbacks. These nets are supervised because using a set of correct input-output pairs, called the training set, small changes in the connection weights are made in order to minimize the difference between the actual and the desired output values in a distributed way. Back propagation is the most popular supervised feed forward network. In the unsupervised recurrent type, the networks allow information to flow in either direction. These models are called unsupervised since the weight matrix is fixed at the beginning using global information and never changed. These networks are useful in optimization applications where a certain cost function should be minimized. One should merely choose a neural network whose energy function coincides with the given cost function. A Hopfield model is the most popular unsupervised recurrent network.

An application of neural network in gravity is in its early stages. We hope to develop a more flexible intelligent method for gravity interpretations with applying other methods in addition of neural networks like Fuzzy Logic, Genetic algorithms in future, specially to develop a near-real-time processing system.

In this paper, we explore the unsupervised recurrent Hopfield network.

3- Hopfield Network

The Hopfield model is a single layer feedback neural network. In this type of neural network the neurons are all connected to each other and the weights of the forward connections are the same as its reverse connection so the data entered in the network have the effects in all of the neurons available. The weight of the neurons connections is fixed and can be calculated by Hopfield methodology. As it has been shown in the FIG.1 it is a 4-neuron Hopfield network diagram.

The energy function of the network may be defied as:

$$E(v)=-1/2 \sum_{i=1}^{n} \sum_{j\neq i=1}^{n} WijViVj - \sum_{i=1}^{n} IiVi \qquad (1)$$

In this work, we follow the error function as energy cost function which should be minimized.

4-Depth estimation of gravity anomalies

The general gravity effect at an observation point (x,z=0) caused by simple body models like sphere and horizontal cylinder centered at x=0 and buried at a depth of z is given (Abdelrahman et al.,2001)by:

$$g= \frac{A}{(x^2+z^2)^q} \quad (2)$$

Where q is a value characterizing the nature of the object:
a) If the object is a horizontal cylinder model q=1
b) If the object is spherical model q=1.5
It is a good estimation for some objects near to spherical or cylindrical shape that the value of q is in the range of 1-1.5.
It is clear from equation (2), that the horizontal location of the object can be obtained from the bouger anomalies contours and residual anomalies contours. For example as shown in FIG.2 it is very clear from the intensity of the colors of bouger contours that where the horizontal location of the object is.

Suppose we have M gravity data measured over an object of unknown amplitude factor A and is located at the position (l).To estimate the unknown amplitude factor, we build a cost function between the measured and calculated gravity anomaly of the model. The theoretical gravity anomaly at a measurement point k can be written:

$$g_k^c = G_{lk} A, \quad (3)$$

Where A is the amplitude factor and G_{lk} represents the geometrical relation between the position l and the observation point k.
There is a problem here that if we have the inexact data due to noise and other sources of errors, the amplitude factor how can be calculated? This can be approximated in a least square method by a solution that minimizes a cost function between the measured and calculated data. We define a cost function C in terms of the some squares of the differences between the measured and calculated data (Salem, et al, 2003):

$$C= \frac{1}{2}\sum_{k=1}^{M}(g_k - g_k^c)^2 = \frac{1}{2}\sum_{k=1}^{M}[g_k - G_{lk}A]^2 \quad (4)$$

Where g_k represents the measured gravity data. The amplitude factor A must be represented in a system consistent with the output the Hopfield network, where a typical bit can be 1 or 0.The amplitude factor can be expressed as:

$$A= \sum_{i=1}^{n=D+U+1`} 2^{i-D-1} b_i \quad (5)$$

D is the number of down bits of the binary value and U is the number of up bits of it. It is clear that D and U are depending on the precision and amplitude, respectively.

Substituting of Eq.(5) into Eq.(4), expanding, and regrouping gives the connection weights and input initial values as mentioned below.

$$(6)\, W_{lij} = -\sum_{k=1}^{M} 2^{(i+j-2D-2)} (G_{lk})^2$$

$$(7)\, I_{ij} = -\frac{1}{2}\sum (2^{(i+j-2D-2)} G_{lk})^2 b_i + \sum 2^{(i-D-1)} G_{lk} g_k$$

So the Hopfield energy to estimate the amplitude factor at the location l becomes:

$$(8)\, E_l(b) = -\frac{1}{2}\sum_{i=1}^{n} \sum W_{ij} b_j b_i - \sum_{i=1}^{n} I_{li} b_i$$

Similar to Salem et al.(2001),the Hopfield network with 9 neurons is used to estimate the amplitude factor at a set of different depths.

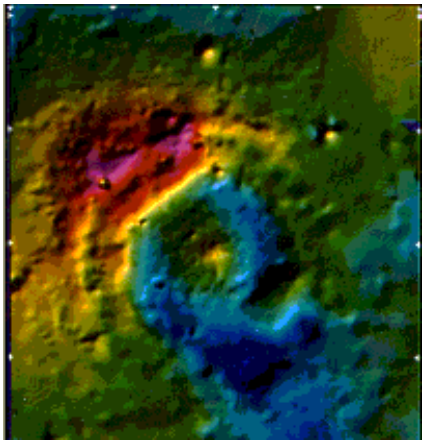

FIG.1:A 4-neuron Hopfield Neural Network

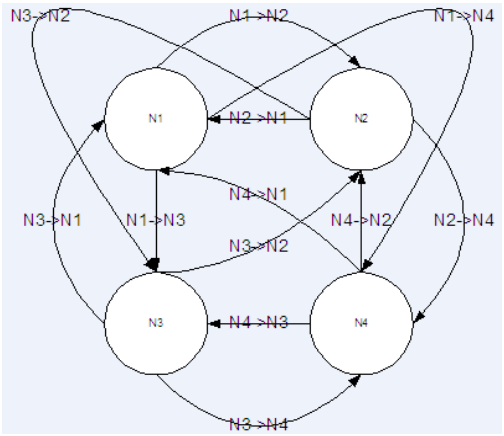

FIG.2: A sample of bouger anomaly[Telford,1976]

5-Synthetic data and the Hopfield network estimations in practical cases

After calculating the weights and biasing values of the network it rotates while get to a stable condition ,it means that after calculating the weights and biasing values they will be fixed but the initial value of depth will applied to the rotating network until get to a condition which its output is the same as the previous output; in this state it is said that the energy of the neural network has got its minimum it is similar to a ball which runs a long a topographic area with valise and tops then it will be stopped in one of the valise that have a minimum depth. So we prepared a Hopfield neural network program that tested it for these different initial values of depth and then this program

calculates the energy of the network in its stable state. So the output of the network which has the least energy means the depth estimation which is near to actual depth of the source.
To test the behavior of the network we fed the noisy data of a cylinder that the ratio of signal to noise was 5, 15 percent. After the network get to the stable states the depth was estimated by the program mentioned before. The results for this test have been presented in the Table 1.
These results are like the one which Ahmed Salem has reported (2003); we also believe that it means that the network has good ability to detect the near surface object in present of other noises like heavy buildings and tunnels or cavities which may be effect on the object near to it.This is a very hard task to distinguish the coefficients of a suitable filter to attenuate the effects of the noise on the main signal but fortunately the artificial neural network is able to have a good result in present of the noise; through the noise is in popular condition an additive one but to detect the noise it is not possible to add an anti aliasing filter to avoid the noise to be added to the main gravity signal.
As we were tested the network we test it for the gravity data measured on the surface of the earth ground on top of a Subterranean canal in the North entrance of Geophysics Institute .It was very interesting that by the Geosoft software the precision was approximately 50 centimeters but the neural network result precision was 10 centimeters.

Table 1: *Dept estimation in present of noise*

Model	***Cylinder***				***Sphere***			
Noise	**5%**		**10%**		**5%**		**10%**	
Parameter	**Z**	**A**	**Z**	**A**	**Z**	**A**	**Z**	**A**
1	**0**	**5**	**0**	**10**	**0**	**5**	**0**	**2.5**
2	**5.5**	**1.5**	**5**	**5**	**0**	**5**	**5**	**2.5**
3	**3**	**1.5**	**6.6**	**7.5**	**3.3**	**0.5**	**6.6**	**3**
4	**2**	**1**	**5**	**1.5**	**2.5**	**0.5**	**5**	**3**
5	**2**	**1.4**	**6**	**1.5**	**2**	**0.5**	**8**	**6**
6	**3**	**0.01**	**3.3**	**1.5**	**1.6**	**0.5**	**5**	**3**
7	**2**	**0.1**	**2.8**	**1.5**	**1.4**	**0.5**	**2.8**	**0.5**
8	**2.5**	**0.1**	**2.5**	**1.5**	**3.7**	**3**	**2.5**	**0.5**
9	**2.6**	**0.1**	**5.5**	**0**	**3.3**	**3**	**2.2**	**0.5**
10	**1**	**1.5**	**1**	**2.5**	**1**	**2.5**	**1.2**	**5**

6-Conclutions

In this paper a new method has been proposed for intelligent interpretation of gravity data for exploration, especially in depth estimations. The observed gravity anomaly of the object is assumed to be produced by an equivalent source of cylinder or sphere, which has an amplitude factor related to the radius, density contrast and depth. WE used the Hopfield neural network to optimize the amplitude factor of the source at a set of subsurface targets. For each target location

we run the network and calculate its stable energy and after that the one which has the minimum energy in its stable state was supposed as the nearest value to actual location and depth .So we tested the network for synthetic data of the two models of sphere and cylinder in present of noise and saw the results have good adaptation to actual values. For a testing of field data we measured the gravity points of the ground in top of a subterranean canal and fed the data corrected to the network to see the depth estimation by the network it was more precise than that of the Geosoft software presented.

It will be our future attempts to develop this method for higher noisy signals especially in a Fuzzy Logic methodology jointed to genetic algorithm to have an access for other complicated shapes of objects.

7-Acknowledgements

We are indebted to Prof. Caro Lucas for all his contribution and kind helps and Prof. Emile E.Klingle and Alexandre A.Gret for their key guidance and scientifically supports.

REFRENCES:

Abdelrahman, E.M, El-Araby, H.M, Al-araby, 2001, Three least squares minimization approach to depth, shape, and amplitude coefficient determination from gravity data, Geophysics,66,1105-1109

Hopfield and Tank, 1985, Neurasl computation of decisions in optimization problems, Biological Cybernetics 52,141-152

Menhaj, Fundamental of artificial neural networks, Amirkabir University Press, 2000

Gupta.O.P., A least squares approach to depth determination from gravity data, Geophysics, vol.48, no3(March 1983),p 357-360

Smith R.A, 1959, Some depth formulae for local magnetic and gravity anomalies, Geophysical Prospecting, 7, 55-63.

Ahmed Salem ,Eslam Elvadi, and Keisuke Ushijima ,Detection of cavities and tunnels from magnetic anomaly data using neural network,Proceeding of the 5th International Symposium,January 2001,Tokyo,pp.377-383.

Charniak and McDermott.1985,Introduction to Artificial Intelligence:Addison-Wesley.

Ahmed Salem ,Eslam Elvadi, and Keisuke Ushijima ,Detection of cavities and tunnels from gravity anomaly data using neural network,Proceeding of the 7th International Symposium,January 2003,Tokyo,pp.200-205

Telford, W.M.Geldart, L.P.Sheriff, 1976, Applied geophysics: London, Cambridge Unive Press.

Mineral chemistry of index minerals and their implications in the genesis of the Baba Ali magnetite skarn deposit, western Iran.

Dr. Hassan zamanian*

zamanian138@yahoo.comUniversity of Lorestan ,Khorram Abad ,Iran

Dr. Amir Pazoki

a_pazoki@yahoo.comUniversity of Lorestan ,Khorram Abad ,Iran

Sayed Aref Alavi

salsf_aba@yahoo.comM.Sc student of Azad University, Khorram Abad ,Iran

Abstract

The Almoughlagh Batholith, consisting chiefly of quartz-syenite and syenogranite rocks, belong to the magnetite series granitoids, are mostly of I- type, metaluminous and calk-alkaline in nature. The batholoth invaded both the Baba Ali diorite and Songor Series culminated in thermal and hydrothermal metamorphic aureoles in which Baba Ali magnetite deposit formed. Petrography and geochemistry of the host rocks and index minerals such as garnet, pyroxene and magnetite reveal a descending temperature regime, beginning at the peak of thermal metamorphism (550^0C) and ending with the main phase of magnetite mineralisation (350-400 ^{0}C) Mineral chemistry of prograde minerals namely garnet and pyroxene implemented to classify the Baba Ali as a typical Fe-Skarn deposit.

Kayword : Almoughlagh , Fe-Skarn , Baba Ali , magnetite , hydrothermal .

Introduction

The Baba Ali magnetite deposit is located in the western Sanandaj-Sirjan Zone of Iran and also on the northeastern slope of the Almoughlagh Mountain(long. 48^0 50'E - 48^0 15'E and lat. 34^0 45' N - 35^0 00 N). The Almoughlagh Batholith forms the Almoughlagh Mountain with an outcrop area of 159.5 sq. km**.** Baba Ali deposit is approachable from Hamadan city (~ 40km, Fig 1).The entire mineralized area forms a complex, referred to as the Hamakassi deposits, constituting of four deposits, namely the Baba Ali, Chenar, Gelali, and Tekyeah deposits , amongest which the Baba

* University of Lorestan ,Khorram Abad ,Iran

Ali happens to be the largest. The estimated ore reserve at the Baba Ali deposit is about 66 mt with a grade of 61% for Fe (Central Iron Ore Co ,1991)[1].

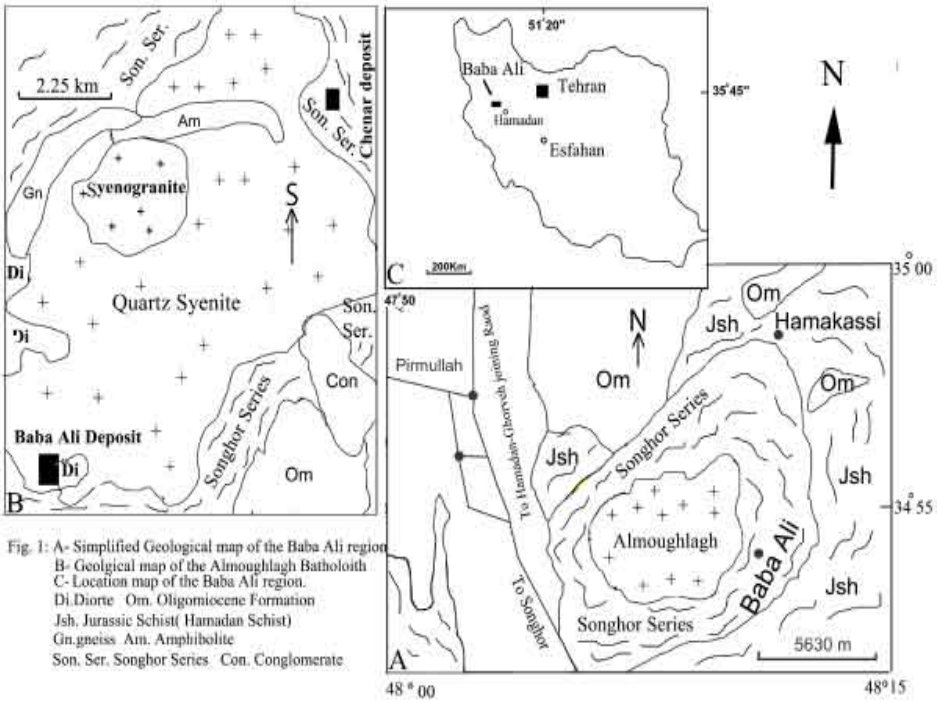

Fig. 1: A- Simplified Geological map of the Baba Ali region
B- Geolgical map of the Almoughlagh Batholoith
C- Location map of the Baba Ali region.
Di.Diorte Om. Oligomiocene Formation
Jsh. Jurassic Schist(Hamadan Schist)
Gn.gneiss Am. Amphibolite
Son. Ser. Songhor Series Con. Conglomerate

Geology setting and petrography

Surrounding the Almoughlagh Batholith the rock formations (Fig 1A) have been subdivided mainly into three main units, namely the Songhor Series (Triassic-Jurassic), Hamadan Schists (Jurassic) and the Limy Formations (Oligomiocene). The Songhor Series is a volcanosedimentary sequence, constituted of alternating schistose and limy lithounits, interbedded with metamorphosed spilitic lava and andesitic tuff (Barud, 1975)[2]. The Songhor Series suffered the regional metamorphism and deformation in three successive orogenic phases, the Late Kimmerian (~136 Ma, Amiri, 1995, Bellon and Barud, 1975)[3] followed by the Laramide (65 Ma, Darvishzadeah, 1992)[4], and the Pasadenian (~2 Ma, Amiri,1995)[5] phases, the latest accompanied by the emplacement of the Almoughlagh Batholith. The Late Kimmerian (Jurassic – Cretaceous) phase metamorphosed the Songhor Series to the greenschist - lower amphibolite facies. Petrological characters of the Almoughlagh batholith have been studied earlier (ValliZadeah and Cantagral, 1975; Amiri, 1995)[6]. These authors described the Batholith as a ring complex, consisting mostly of quartz syenite porphyry, gabbro and diorite. Towards the eastern and southern margins of the Batholith, the rocks were reported to grade into gneiss with amphibolitic enclaves. Other authors have referred to the entire Batholith as the Almoughlagh diorite (Berberian and King, 1981)[7]. The present work revealed that the Almoughlagh Batholith

is a complex body, constituted chiefly of quartz syenite and syenogranite (Fig 1) groups as mapable petrographic units. The areal spread of quartz syenite group is far extensive and in them one comes across remnant enclaves of meta-dioritic rocks. The modal composition varies from quartz syenite to quartz alkali-syenites to alkali-syenite and quartz-monzonite(Fig2).

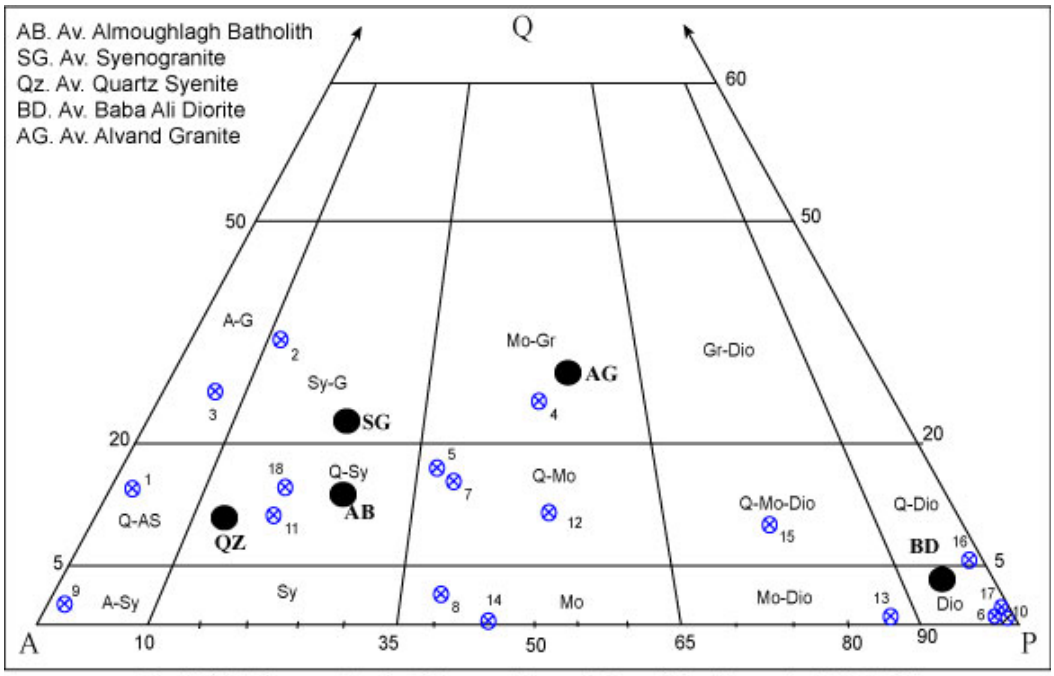

Fig. 2 QAP diagram showing Petrographic variations of the Almonglagh Batholith-

Small enclaves of Baba Ali metadiorite occur within and on the margins of the Almoughlagh Batholith. They represent the unassimilated or unskarnized rocks which were subjected to regional metamorphism along with the Songhor Series. Petrographically, these rocks reveal relict igneous texture, are medium to coarse grained, consisting of phenocrysts of plagioclase (andesine to laboradorite) within the groundmass of tiny plagioclase, quartz and hornblende. Most skarn deposits of economic importance are formed in the contact metamorphic aureoles of intrusions of dioritic to granitic plutons in orogenic belts (Einaudi and Burt, 1982)[8].

Zoning

In the Baba Ali magnetite skarn deposit the main load of magnetite ore body lies between the dioritic and quartz syenitic rocks of the Batholith, hosted mainly by the meta-dioritic rocks.(Fig1). Petrographically, one comes across a mineralogical zoning between the meta-dioritic rocks that show the effects of deformation only, to reaction zones in which new mineral assemblage was formed. From SE towards NW, eight such zones with distinct mineral assemblage have been recognized, away from the Almoughlagh quartz syenite (Fig3).

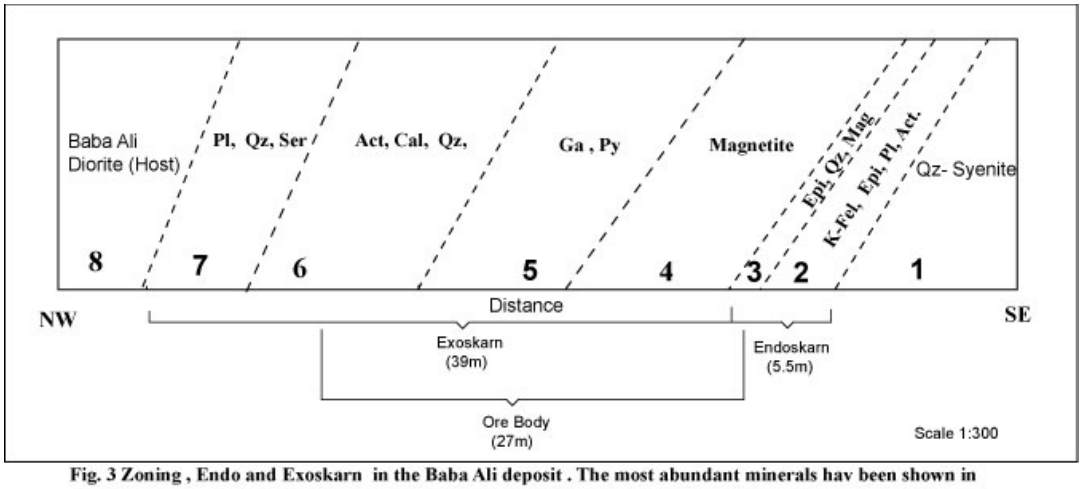

Fig. 3 Zoning , Endo and Exoskarn in the Baba Ali deposit . The most abundant minerals hav been shown in each zone .

Mineralogy and Mineral chemistry of the index minerals (Garnet, Pyroxene and magnetite)

Zone 5 is the most informative zone of the Baba Ali skarn deposit, since it gives an opportunity to establish the intensity of thermal metamorphism before the rocks suffered hydrothermal veining and mineralisation. It is characterized by the index minerals like garnet, pyroxene and magnetite and preserves the skarn mineral assemblage beyond the zone of magnetite mineralisation. Garnet occurs as coarse, idiomorphic, stout grains and short prismatic grains, showing intergrowth with pyroxene . No zoning was observed either in garnet or in the pyroxene grains and neither of these minerals showed any inclusions. Microscopic as well as electron micro-probe analysis revealed the garnet composition (Table1 ,Fig 4) as andradite (35 to 92 mol% andradite**).** Pyroxene also occurs as short idiomorphic to subhedral grains and rarely as long prismatic grains. Compared to garnet the pyroxene forms relatively coarser grains and the EMP investigation revealed the composition (Table 2,Fig 4) in the salite range (Di_{66} Hed_{44} to Di_{53} Hed_{47}). The $Fe_{(t)}/(Fe_{(t)} + Mg)$ ratio in the salite shows a narrow range between 0.36 to 0.44 while the $Fe_{(t)}/(Fe_{(t)} + Al)$ ratio in the co-existed garnet shows a very broad range between 0.23 to 0.98. It is evident that the two minerals were formed at the threshold temperature of incorporating more and more iron in the garnet composition. Magnetite is whitish gray without any anisotropy or exsolution product, indicating lack of any mix-crystal development (Ramdohr, 1980)[9]. This observation is also consistent with the EMP analyses (Table 3) of magnetite samples showing a rather pure magnetite phase, devoid of impurities such as Mg, Mn, Zn, Ni, Ti, V, and Cr, which get readily incorporated in magnetite formed at high temperature. Magnetite occurs as idiomorphic, equigranular massive grains, as vein mineral filling open spaces and substituting pre-existing minerals like garnet, pyroxene, calcite, plagioclase, amphibole and epidote.

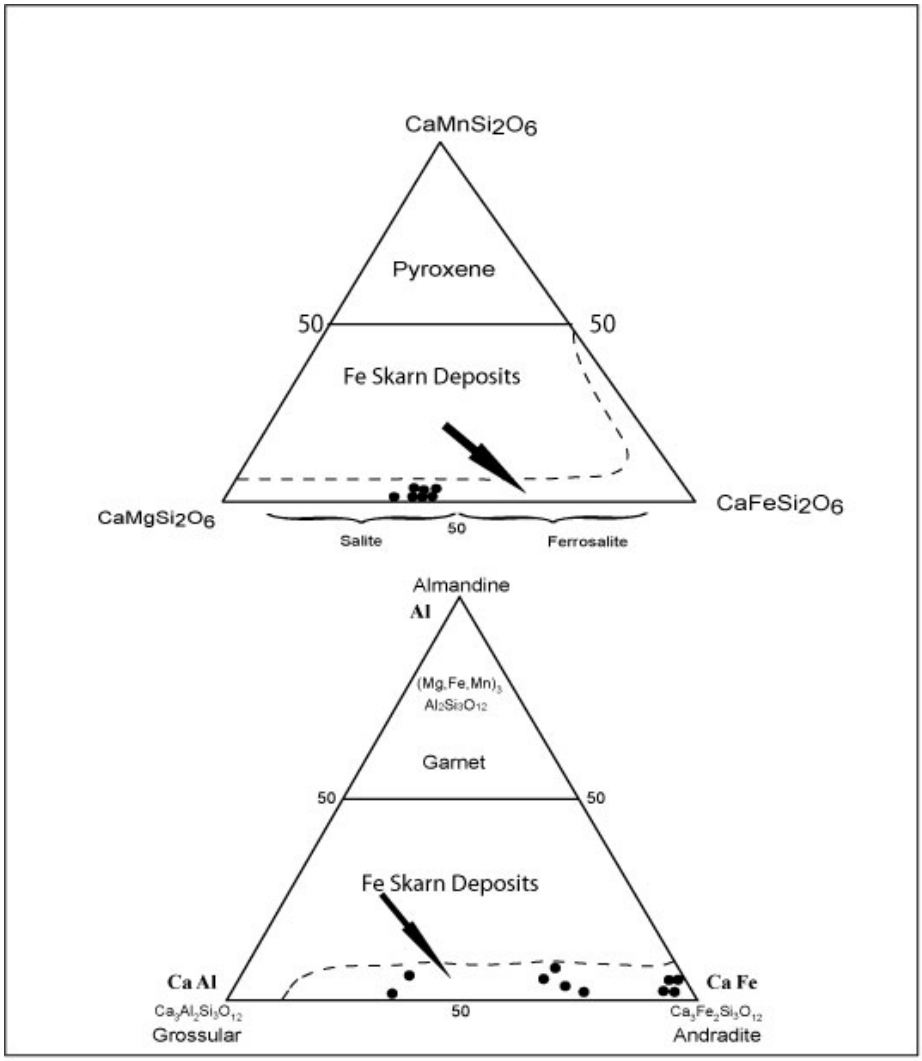

Fig. 4 Compositions of garnet and pyroxene for Baba Ali Iron Skarn deposit.

Table (1) EMP analysis of garnets from Baba Ali deposit

Sample	Na_2O	K_2O	CaO	SiO_2	Al_2O_3	MgO	FeO(T)	MnO	Cr_2O_3	TiO_2	Total	Fe Mol%	Mg Mol%	Mn Mol%
Bc.6.c4	0.346	0.019	24.132	50.98	0.688	10.404	11.45	0.48	0.00	0.032	98.54	0.124	0157	0.005
Bc.6.c7	0.213	0.000	15.08	52.78	0.31	11.713	9.512	0.407	0.00	0.033	100.05	0.103	0.176	0.004
Bc.6.c8	0.228	0.00	24.55	50.95	0.32	10.79	10.199	0.43	0.047	0.027	97.565	0.11	0.162	0.004
Bc.6.c12	0.306	0.023	22.46	51.94	0.401	10.71	11.113	0.46	0.007	0.028	99.541	0.12	0.167	0.005
Bc.6.c14	0.36	0.001	23.24	51.02	0.49	10.68	10.89	0.65	0.00	0.035	97.366	0.118	0.164	0.007
Bc.c.617	0.312	0.034	23.44	50.43	0.43	11.52	11.11	0.54	0.002	0.029	98.62	0.12	0.173	0.005
Bc.6.c18	0.44	0.007	26.11	52.33	0.32	10.89	9.03	0.72	0.003	0.04	99.89	0.097	0.136	0.007

Table (2) EMP analysis of pyroxenes from Baba Ali deposit .

Sample	Na_2O	K_2O	CaO	SiO_2	Al_2O_3	MgO	FeO(T)	MnO	Cr_2O_3	TiO_2	Total	Fe Mol%	Mg Mol%	Mn Mol%
Bc.6.2	0.009	0.02	34.76	36.03	5.037	0.22	21.47	0.35	0.00	0.37	98.28	0.10	0.003	0.003
Bc.6.3	0.00	0.00	23.752	36.48	20.90	0.20	13.97	0.09	0.012	0.045	95.3	0.067	0.003	0.009
Bc.6.9	0.00	0.08	35.33	35.60	7.57	0.27	18.47	0.36	0.26	0.46	98.18	0.09	0.004	0.003
Bc.6.11	0.00	0.002	23.78	37.05	21.415	0.03	13.01	0.025	0.00	0.07	95.4	0.06	0.003	0.000
Bc.6.14	0.00	0.00	34.60	34.61	5.52	0.14	21.20	0.00	0.00	0.24	96.4	0.10	0.002	0.00
Bc.c.15	0.043	0.00	33.27	34.25	0.47	0.23	26.63	0.20	0.022	0.09	95.3	0.13	0.0032	0.002
Bc.6.c16	0.00	0.00	33.71	35.01	0.44	0.24	26.86	0.315	0.00	0.00	96.6	0.13	0.0035	0.003
Bc.6	0.00	0.025	33.65	34.817	0.48	0.26	26.68	0.27	0.0	0.035	96.2	0.13	0.004	0.002
Bc.6.18	0.02	0.00	35.16	34.61	6.38	0.28	18.34	0.26	0.12	0.64	95.74	0.09	0.004	0.0002
Bc.6.19	0.092	0.036	34.50	35.64	6.67	0.35	17.88	0.38	0.031	0.46	96.00	0.08	0.0052	0.004

Table (3) EMP compositions of magnetite from the Baba Ali deposit.

Al_2O_2	MgO	FeO(t)	MnO	TiO_2	Cr_2O_3	NiO	CoO	ZnO	V_2O_5	Total
0.128	0.28	86.59	0.00	0.007	0.009	0.046	0.000	0.000	0.022	86.83
0.58	0.095	71.82	0.000	0.000	0.098	0.00	0.00	0.00	0.00	72.58
0.096	0.020	85.50	0.000	0.06	0.000	0.00	0.00	0.00	0.026	85.70

Conclusion

The compositions of pyroxene and garnet that fall well within the field recognized (Meinert, 1992)[10] for these minerals from Fe skarns show that the Baba Ali deposit can be classified as Fe skarn deposit. (Fig 4).The main phase of Fe mineralisation in the present case did not accompany the crystallization of phases like andradite and salite during the peak temperature of skarnization. A descending trend of temperature (550 –350 ^{0}C), beginning with the formation of garnet-pyroxene assemblage and ending with the magnetite mineralisation can therefore be assumed during the skarnization and mineralisation. The main phase of Fe mineralisation occurred in the temperature range of 350 – 400^{o} C, since the lower temperature limit for formation of calcic skarn is held to be 350^{o} C (Zharikov, 1970, p.635)[11]. The magnetite mineralisation represents therefore a low temperature facies. Magnetite mineralisation in hydrothermal conditions related to igneous intrusions of intermediate composition has been reported form many a region around the Pacific (Guilbert and Park, 1986, 455)[12]. The iron mineralisation in Baba Ali skarn deposit with a limited extent of thermal aureole, extensive exoskarn and association of hydrothermal minerals with magnetite should have taken place at shallow (mesoabyssal) depth.

References

[1] Central Iron Ore Co.,1991, Preliminary exploration of Hamakassi iron Deposits, 134p (in Persian).

[2] Barud, J, 1975, Geological Map of the Kermanshahan Quadrangle (1:250000) Published by Geol. Surv. of Iran, Tehran.

[3] Bellon, H. and Barud, J.,1975, Donnes nouvellexs sur le domaine metamorphique du Zagros (Zone de S-S au niveau de Kermanshah-Hamadan(Iran); Nature, age et interpretation des series metamorphiques et des intrusious, evolution structurale. Fac, Sci. d'orsay, Paris 14p. (In French)

[4] Darvishzadeh, A., 1992, Geology of Iran. Nashre Danesh , Tehran, Iran, 901p (in Persian).

[5] Amiri, M.,1995, Petrography of the Almouglagh. Unpublished M.Sc Thesis, University of Tarbiat-e- Moalem, Tehran, Iran, 231p(in Persian).

[6] Valizadeah, M.V. and Cantagral, J.M., 1975, Premieres donnees radiometrique (K-Ar et Rb-Sr) sur les- micas du complex magmatique du mont Alvand. Pres Hamdan (Iran Occidental) Comptes, Acad. Des Sci. Paris, Ser. D, v. 281, p.1083-1086. (in French)

[7] Berberian, M. and King, G.C.P.,1981, Towards a Palaeogeography and tectonic evolution of Iran. Can. Jour. Earth Sci., v.18, p.210-265.

[8] Einaudi, M.T., and Burt, D.M., 1982, Introduction - terminology, classification, and composition of skarn deposits. Econ. Geol. v., 77, p.

[9] Ramdohr, P.,1980, The ore minerals and their intergrowth, 2nd ed., Intern. Ser. in Earth Sci ., v.35. London. Pergamon Press, 1205 p.

[10] Meinert,L.D.(1992) Skarns and skarn deposits. Geosc. Can,V19,PP145-162.

[11] Zharikov, V.A.,1970, Skarns: Part I., II., and III, Int'l. Geol. Rev., v.12, p.541-559, p.619-647, p.760-775.

[12] Guilbert,J.M and Park,Jr.C.F.(1986)The geology of ore deposits .W.H.Freeman and company.985P.